

IMAGEDIT: LET ANY SUBJECT TRANSFORM

Fei Shen^{1*}, Weihao Xu^{2*}, Rui Yan², Dong Zhang³, Xiangbo Shu², Jinhui Tang^{2,4}

¹National University of Singapore; ²Nanjing University of Science and Technology

³Hong Kong University of Science and Technology; ⁴Nanjing Forestry University

<https://muzishen.github.io/IMAGEDit/>

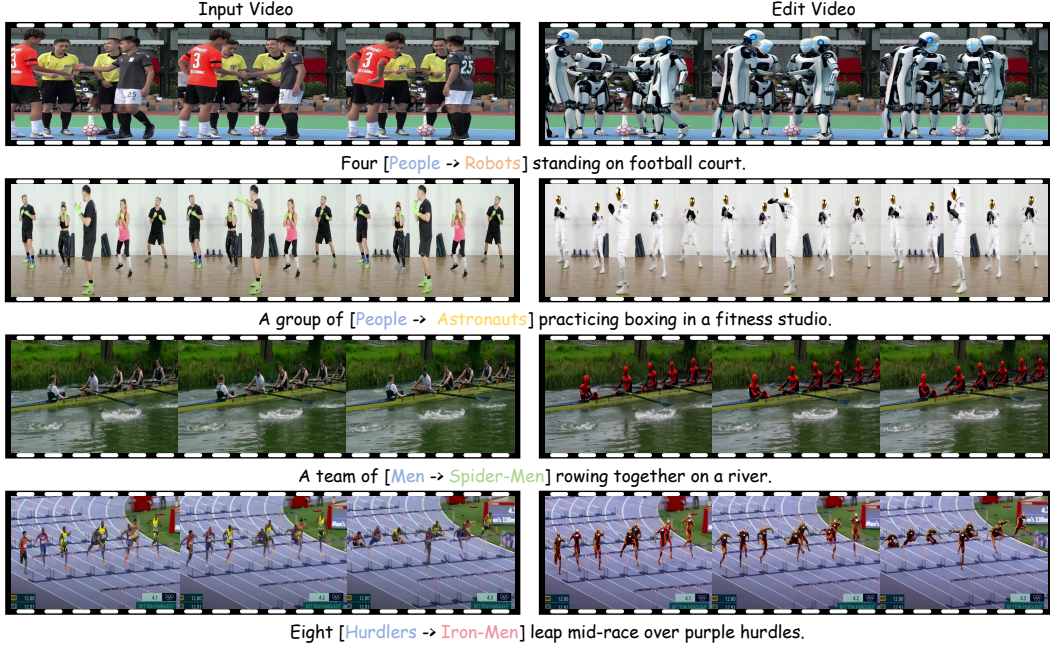


Figure 1: **Visualization results of IMAGEDit.** Given any video with any number of designated subjects, IMAGEDit performs precise category transformations while maintaining subject count and spatial layout. Especially in crowded scenes with overlapping subjects, IMAGEDit demonstrates stable consistent editing.

ABSTRACT

In this paper, we present **IMAGEDit**, a training-free framework for any number of video subject editing that manipulates the appearances of multiple designated subjects while preserving non-target regions, without finetuning or retraining. We achieve this by providing robust multimodal conditioning and precise mask sequences through a prompt-guided multimodal alignment module and a prior-based mask retargeting module. We first leverage large models' understanding and generation capabilities to produce multimodal information and mask motion sequences for multiple subjects across various types. Then, the obtained prior mask sequences are fed into a pretrained mask-driven video generation model to synthesize the edited video. With strong generalization capability, IMAGEDit remedies insufficient prompt-side multimodal conditioning and overcomes mask boundary entanglement in videos with any number of subjects, thereby significantly expanding the applicability of video editing. More importantly, IMAGEDit is compatible with any mask-driven video generation model, significantly improving overall performance. Extensive experiments on our newly constructed multi-subject benchmark MSVBench verify that IMAGEDit consistently surpasses state-of-the-art methods. Code, models, and datasets are publicly available at <https://github.com/XWH-A/IMAGEDit>.

*Equal contribution.

1 INTRODUCTION

“Any subjects can transform together.” -Many people voiced this wish as children while watching films, animations, and live performances. Television media often have such applications (Shen et al., 2025), e.g., the coordinated team transformation in *Ultraman*¹ and the multi subjects synchronized transformation in *Sailor Moon*². Reproducing this effect in real videos typically requires specialized equipment and extensive character modeling, increasing cost and limiting generalization. In this work, to *let any subject transform* while preserving non-target regions, we propose a novel, training-free framework for video editing with any number of subjects. As shown in Figure 1, even in scenes with any number of subjects where spatial relations are complex and interactions are dense, conditions that differ markedly from single or few subject settings of existing methods (Wu et al., 2023; Ceylan et al., 2023), our framework performs the edits reliably and achieves remarkable results.

With the rapid progress of generative models, video editing (Wu et al., 2023; Ceylan et al., 2023) has advanced substantially, driven by generative adversarial networks (Radford et al., 2015; Goodfellow et al., 2020; Donahue et al., 2016; Odena et al., 2017) and diffusion models (Rombach et al., 2022; Ramesh et al., 2022; Shen et al., 2025). However, most existing approaches (Geyer et al., 2023; Wang et al., 2025; Ceylan et al., 2023; Ku et al., 2024) focus on single or at most two subjects and typically rely on either task-specific training or precise guiding masks, which limits their generalization ability. For instance, as seen in the first row of Figure 2, although existing methods can achieve accurate editing in terms of position and quantity with precise masks, the subject categories do not faithfully reflect the editing prompt, highlighting limitations in the edited conditions. In multi-subject scenarios with dense layouts and heavy occlusions, these methods often become unstable, degrading perceptual quality. As shown in the second row of Figure 2, boundary entanglement in segmentation (Ren et al., 2016; He et al., 2017) can cause edits to spill across subjects, misplacing attributes, such as a dog head on a robot wolf body. Due to limited compositional grounding of prompts and control conditions, attention is diluted across subjects, leading to temporal inconsistency and disrupting edit continuity. In summary, editing videos with many subjects is more challenging than single or few subject cases. Occlusion and boundary entanglement make segmentation, tracking, and identity preservation error-prone, while instructions and control conditions must be accurately grounded to multiple subjects to avoid attention dispersion and ensure consistent edits and temporal coherence.

To address these limitations, we propose **IMAGEDit**, a training-free video editing framework that transforms any number of subjects in arbitrary videos without additional training. As shown in Figure 1, IMAGEDit delivers robust and precise edits across subjects of any number and is particularly effective in cases with boundary entanglement. This is achieved through three components: (i) a prompt-guided multimodal alignment module, (ii) a prior-based mask retargeting module, and (iii) a mask-driven video generation model.

In our prompt-guided multimodal alignment module, we first extract the subjects to be edited from the prompt and input a pretrained text-to-image (T2I) model (Rombach et al., 2022; Podell et al., 2023; Chen et al., 2023) to obtain the target appearance. We then feed both the editing prompt and the visual prior into a vision language model (VLM) (Achiam et al., 2023; Wang et al., 2024; Chen et al., 2024) to produce aligned multimodal conditions, namely an expanded text condition and an expanded image condition. For the second component, we present a theoretical algorithm to capture per-frame mask state changes and generate a temporal continuous mask motion sequence aligned with the input video. Finally, for the third component, we input the multimodal conditions and the

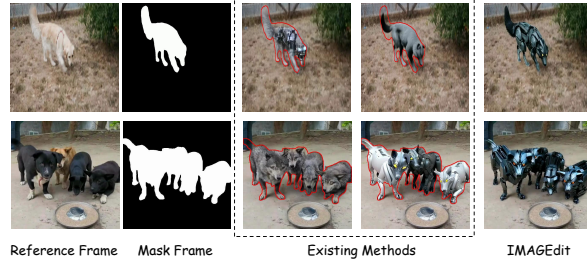


Figure 2: Visual results generated from current video editing methods and our IMAGEDit (Dogs → Robot Wolves). Previous methods apparently retain the reference dog’s appearance. In contrast, the result of IMAGEDit both aligns the robot wolf’s features and captures the reference dog’s layout.

¹[https://en.wikipedia.org/wiki/Ultraman_\(manga\)#Anime](https://en.wikipedia.org/wiki/Ultraman_(manga)#Anime)

²https://en.wikipedia.org/wiki/Sailor_Moon#Live-action_film_&_series

continuous mask sequence into a pretrained mask-driven video generation model to transform the video. From Figure 2, IMAGEEdit achieves reliable and coherent video edits by supplying multi-modal conditions and retarget masks. Moreover, IMAGEEdit operates as a plug in and is compatible with any mask-driven video generator, markedly improving multi subject editing performance, with experimental analysis in Sec. 4.2.

In addition, to address the lack of a benchmark for editing videos with any number of subjects, we construct MSVBench, which comprises 100 cases covering diverse subject counts and scene complexities. Qualitative and quantitative evaluations on MSVBench show that IMAGEEdit delivers strong video editing performance and surpasses existing methods particularly in multi subject settings. Ablation studies further validate the effectiveness and advantages of the framework, offering valuable insights for the community. We also release IMAGEEdit results on multi subject videos, providing a practical solution for research and applications in video editing.

Our main contributions are summarized as follows:

- We propose IMAGEEdit, a novel training free video editing framework that enables the transformation of any number of subjects in arbitrary videos.
- IMAGEEdit generates robust multimodal conditions and precise mask sequences for any number of subjects, offering a promising solution to the community for video editing.
- IMAGEEdit can be seamlessly integrated as a plug in with any mask driven video generation model, consistently enhancing its performance in multi subject scenarios.
- We establish MSVBench, a benchmark with varying subjects for comprehensive evaluation. Experiments on MSVBench show that IMAGEEdit outperforms SOTA approaches.

2 RELATED WORK

Video editing. Early video editing methods mainly relied on GANs (Goodfellow et al., 2020; Mittal et al., 2017; Pan et al., 2017; Li et al., 2018), performing subject edits through warping and rendering pipelines. In recent years, latent diffusion models((Rombach et al., 2022; Peebles & Xie, 2023; Ruiz et al., 2023))have markedly improved the quality and efficiency of image generation. Building on this progress, several works fine-tune T2I models (Wu et al., 2023; Qi et al., 2023; Liu et al., 2024a; Zhang et al., 2025) with spatiotemporal attention on paired samples from a single video to achieve stylization and subject replacement. However, current one-shot training tends to overfit the given sample and fails to align with other target scenes; the issue is exacerbated in unseen, multi-subject, high-density settings, thereby limiting the generalization ability. Meanwhile, another line of research (Wang et al., 2025; Yang et al., 2025; Jiang et al., 2025; Bian et al., 2025) leverages highly scalable conditions, such as instance segmentation masks, to strengthen spatial localization and motion constraints. Yet, this approach inherently depends on masks and is restricted in multi-subject scenarios with overlapping and intertwined instances. To overcome these limitations and truly *let any subject transform*, this paper adopts a mask-driven video editing paradigm that provides precise retargeted mask sequences, enabling high-fidelity and robust any subject video editing.

Instant Segmentation. Instance segmentation aims to produce pixel-level masks for all objects in an image while distinguishing individual instances. Early approaches (Rother et al., 2004) constructed masks for region proposals and refined them iteratively to match instance extents. With the rise of deep networks, one line of work (Ren et al., 2016; He et al., 2017; Li et al., 2017) performs direct regression of instance masks using coarse-to-fine cascade networks. At the same time, another (Zhang et al., 2021; Cheng et al., 2021; 2022)predicts per-instance mask heatmaps or query embeddings for indirect regression, improving accuracy. Recently, prompted segmentation (Kirillov et al., 2023; Ravi et al., 2024; Ren et al., 2024) has been introduced with larger datasets and foundational models to enhance cross-domain generalization. Nevertheless, these methods (Rother et al., 2004; Ren et al., 2016) still struggle in dense scenes due to the supervised training paradigm and annotation constraints, particularly with many subjects. To this end, we adopt a prior-based mask retargeting module that exploits spatial semantic correspondences in deep features and strong generalization, providing precise and temporal consistent instance masks for any number of subjects.

Text to Video Generation. In recent years, image-to-video (I2V) generation (Singer et al., 2022; Yang et al., 2024b) has attracted considerable attention due to its potential in image animation

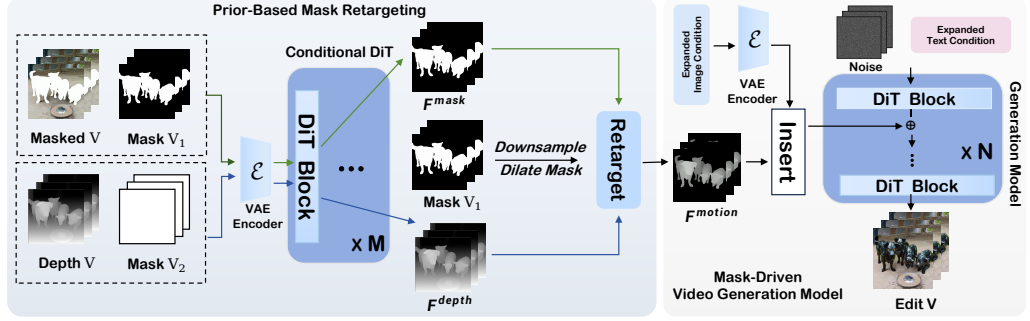


Figure 3: The IMAGEDit framework first derives robust multimodal cues via a prompt-guided multimodal alignment. Then, a prior-based mask retargeting module produces a time-consistent mask sequence aligned with the input video. Finally, the multimodal cues and mask sequence are fed into a video generation model to synthesize the edited video.

and video synthesis. Prior work (Guo et al., 2023) leveraging diffusion models’ strong representation and synthesis capabilities for image inserts temporal layers into pretrained two-dimensional U-Nets (Ronneberger et al., 2015) and fine-tunes with video data to convert static images into dynamic sequences. For example, VideoPainter (Bian et al., 2025) is a dual-branch framework that integrates with video diffusion transformers to achieve robust arbitrary-mask video inpainting. In parallel, specialized I2V frameworks (Singer et al., 2022; Ho et al., 2022) trained from scratch on large-scale, high-quality datasets have demonstrated strong competitiveness. DiT-based I2V approaches (Hong et al., 2022; Yang et al., 2024b; Wan et al., 2025; Gao et al., 2025)) have recently become increasingly popular for their improved global coherence and controllability. Guided by these considerations, we adopt Wan2.1 (Wan et al., 2025) as the base I2V model in this work.

3 METHOD

The overall framework of IMAGEDit is shown in Figure 3. We first introduce the diffusion transformer basics in Sec. 3.1, followed by a description of the three core components in Sec. 3.2: prompt-guided multimodal alignment, prior-based mask retargeting, and the video generation model.

3.1 PRELIMINARIES

In IMAGEDit, we adopt Wan2.1 (Wan et al., 2025) as the base model for mask-guided matching, which comprises a variational autoencoder (Kingma & Welling, 2013), a umT5 text encoder (Chung et al., 2023), and a denoising diffusion transformer (DiT) (Peebles & Xie, 2023). While DiT variants have shown strong performance in image synthesis, DiT based pipelines for video editing remain relatively underexplored compared with UNet based counterparts, particularly in multi subject, mask conditioned settings. Unlike approaches (Geyer et al., 2023; Qi et al., 2023; Yatim et al., 2024) that rely on UNet (Ronneberger et al., 2015), DiT uses a Transformer backbone to model the diffusion process and to capture long range dependencies and global context. Let $x_0 \in \mathbb{R}^{H \times W \times C}$ denote a clean image with height H , width W , and channels C . The forward diffusion process gradually corrupts x_0 into $\{x_t\}_{t=1}^T$ over T discrete steps by adding independent Gaussian noise $z_t \sim \mathcal{N}(0, I)$, where I represents the identity matrix:

$$x_t = \sqrt{\alpha_t} x_{t-1} + \sqrt{1 - \alpha_t} z_t, \quad t = 1, \dots, T, \quad (1)$$

where $\alpha_t \in (0, 1)$ is the variance preserving noise schedule at step t . The reverse diffusion process iteratively removes noise to recover x_{t-1} from x_t . We model this step with $p_\theta(x_{t-1} | x_t)$, which represents the conditional probability distribution of the less noisy image x_{t-1} given the more noisy image x_t :

$$p_\theta(x_{t-1} | x_t) = \mathcal{N}(x_{t-1}; \mu_\theta(x_t, t), \Sigma_\theta(x_t, t)), \quad (2)$$

where $\mu_\theta(x_t, t)$ and $\Sigma_\theta(x_t, t)$ are the mean and covariance predicted by the DiT with parameters θ .

3.2 IMAGEDIT: LET ANY SUBJECT TRANSFORM

Reviewing the results in Figure 2, we observe remarkable variance in editing performance across different subject counts and boundary complexities. A robust mask generation mechanism that can handle multiple interacting subjects is essential for achieving high-fidelity video editing. Prior approaches either rely on supervised segmentation models trained on annotated data, expand dataset

diversity to improve generalization, or introduce new regularization terms to enhance mask consistency. However, under a supervised training paradigm, these methods still struggle to generalize to unseen categories and densely entangled multi-subject scenarios, often leading to boundary entanglement and temporal instability. To address this, we propose a prompt-guided multimodal alignment module that combines textual and visual priors to generate robust editing conditions. In addition, we introduce a prior-based mask retargeting module that produces temporal consistent mask motion sequences across frames. Finally, a mask-driven video generation model is employed to synthesize high-fidelity and robust multi-subject video edits.

Prompt-Guided Multimodal Alignment.

Recent studies (Yin et al., 2023; Singer et al., 2022) show that limited understanding ability of text encoders in video editing models often causes inconsistencies between editing results and the intended semantics when using naive text prompts. In multi subject editing scenarios, this issue becomes more pronounced. From Figure 4 (a) top row, neighboring subjects dilute attention, and a naive prompt fails to impose a clear constraint on “astronaut,” thus not triggering the intended edit. Another case is shown in Figure 4 (a) bottom row, where insufficient textual semantic constraints cause a semantic mismatch, making “Goku”, related attributes only partially take effect on the target. These observations indicate that multi-subject settings require stronger multimodal alignment and subject-level control to ensure precise binding of editing intent and temporal stability. Based on these observations, we introduce a prompt-guided multimodal alignment module to explicitly realize cross-modal alignment and produce stable multimodal conditions.

Specifically, as shown in Figure 5, we first extract subject specific tokens W_{ref} from the original editing prompt P_{edit} . These tokens query a pretrained text to image model (Podell et al., 2023) to generate a visual prior I_{ref} , which bridges the abstract textual description and a concrete visual instance, anchoring the subject’s appearance. Next, we feed I_{ref} and P_{edit} into a vision language model (VLM) (Achiam et al., 2023; Wang et al., 2024). Using an extended instruction template P_{temp} , the VLM aligns the two modalities by interpreting the visual attributes in I_{ref} and expanding the description in P_{edit} in a controlled manner. This yields an enriched and visually grounded textual condition P_{target} :

$$P_{target} = \Phi_{VLM}(P_{edit}, I_{ref} | P_{temp}), \quad (3)$$

where Φ_{VLM} denotes the VLM function that reconciles the semantic intent in P_{edit} with the structure and appearance priors provided by I_{ref} . As shown in Figure 4 (b), grounding the textual expansion in explicit visual evidence improves the fidelity of subject attributes and mitigates attention dilution and semantic drift, resulting in more coherent and targeted video edits.

Prior-Based Mask Retargeting. The accuracy of masks directly determines the controllability and temporal stability of mask-driven video editing. In dense multi subject scenes, general segmentation models such as the SAM family often fail to produce precise instance level masks that distinguish overlapping or adjacent objects, and they cannot capture the hierarchical and occlusion order among subjects, leading to mask leakage and blurred boundaries; these errors further propagate and amplify over time, as shown in Figure 6 (a). To address this, we propose a prior-driven mask retargeting module: constrained by depth priors, it spatially reestimates instance boundaries according to near-

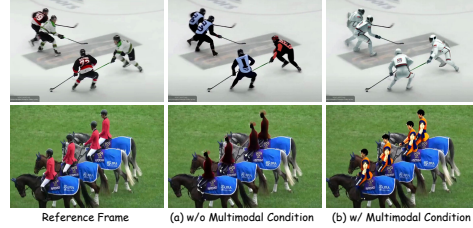


Figure 4: Visualization of the without (w/o) and with (w/) multimodal condition. The first row: Hockey Players → Astronauts; the second row: Horse Riders → Gokus.

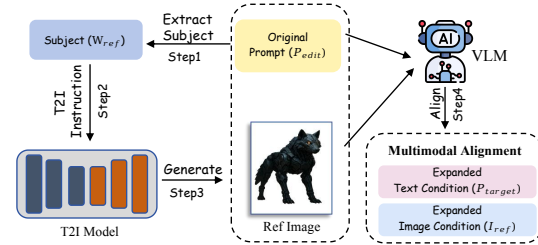


Figure 5: Illustration of prompt-guided multimodal alignment. We generate aligned extended text conditions and extended image conditions for each original prompt.

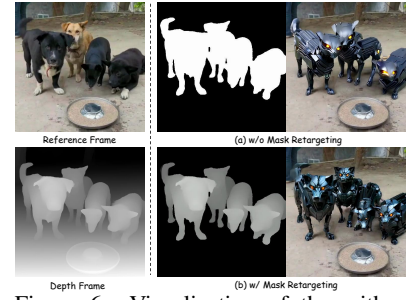


Figure 6: Visualization of the without (w/o) and with (w/) mask retargeting (Dogs → Robot Wolves).

far relationships and temporal generates a retargeted mask motion sequence by enforcing consistency across adjacent frames. This sequence explicitly encodes hierarchical boundaries and occlusion relationships between subjects, significantly reducing mask leakage and improving cross-frame consistency, as shown in Figure 6 (b). As shown in Figure 3, we consider an original video $V_{\text{ori}} = \{v_1, v_2, \dots, v_N\}$ with N frames, where $v_i \in \mathbb{R}^{H \times W \times C}$. We denote the binary instance masks across frames by $M = \{m_1, m_2, \dots, m_N\}$ with $m_i \in \{0, 1\}^{H \times W}$ specifying the editing region for frame i . Similarly, let $D = \{d_1, d_2, \dots, d_N\}$ with $d_i \in \mathbb{R}^{H \times W \times C}$ denote the estimated depth maps. From these inputs, we extract guidance features using a conditional DiT. To obtain the mask-guided features F^{mask} , we first compute a masked video via element-wise multiplication with the binary mask: $V_{\text{masked}} = V_{\text{ori}} \odot M$. Each masked frame from V_{masked} is then concatenated with its corresponding binary mask m_i along the channel dimension and fed into the conditional DiT. The resulting output sequence is defined as $F^{\text{mask}} = \{F_i^{\text{mask}}\}_{i=1}^n$. Similarly, to get the depth-guided features F^{depth} , each depth map d_i is concatenated with an all-ones mask and processed by a similar DiT architecture, yielding $F^{\text{depth}} = \{F_i^{\text{depth}}\}_{i=1}^n$. Subsequently, we achieve precise redirection of the mask region by injecting depth features F^{depth} into the editing area. To ensure the depth information is fully integrated into the target area, avoiding missing or discontinuous information during feature fusion, and to provide a smooth transition for the fusion of depth features and mask features mask in the conditional module, we apply morphological dilation to the initial editing mask to expand the editing region. Formally, for each frame mask m_i , the dilated mask is

$$m'_i[p, q] = \max_{(u, v) \in \mathcal{N}_k} m_i[p + u, q + v], \quad (4)$$

where $\mathcal{N}_k = \{(u, v) \mid -r \leq u, v \leq r\}$ is a square neighborhood of size $k \times k$ with radius $r = \lfloor k/2 \rfloor$. This dilation enlarges the foreground to provide a blending margin. We then apply a Gaussian filter to m'_i and downsample the result to obtain a soft mask \tilde{m}_i . Collectively, the final softened and resized mask sequence is $\tilde{M} = \{\tilde{m}_1, \tilde{m}_2, \dots, \tilde{m}_N\}$. Let the final motion guidance sequence be $F^{\text{motion}} = \{F_i^{\text{motion}}\}_{i=1}^n$. At each spatial location (x, y) we compute

$$F_i^{\text{motion}}(x, y) = \tilde{m}_i(x, y) F_i^{\text{depth}}(x, y) + (1 - \tilde{m}_i(x, y)) F_i^{\text{mask}}(x, y). \quad (5)$$

This design ensures that within subject regions (where \tilde{m}_i is high), editing is primarily guided by depth to recover geometry and proper layering, while in background regions (where \tilde{m}_i is low), mask constraints dominate to preserve appearance and temporal stability.

Video Generation Model. Given the retargeted mask motion sequence F^{motion} , we can condition any mask-driven video generator by attaching a ControlNet style branch to a ViT backbone (Wan et al., 2025; Gao et al., 2025; Zhang et al., 2023; Jiang et al., 2025). Although F^{motion} can in principle be injected at all denoising steps, continuing the fusion at late steps produces severe artifacts and unnatural seams, because early steps shape low frequency structure while late steps refine high frequency details (Wu et al., 2024; Qian et al., 2024). We therefore inject only in the early structural phase and revert to mask only conditioning for refinement. Let T be the total number of steps and τ the injection threshold. With depth guided features $F_{i,t}^{\text{depth}}$ and mask guided features $F_{i,t}^{\text{mask}}$, the conditional feature is

$$F_{i,t}^{\text{cond}}(x, y) = \begin{cases} \tilde{m}_i(x, y) F_{i,t}^{\text{depth}}(x, y) + (1 - \tilde{m}_i(x, y)) F_{i,t}^{\text{mask}}(x, y), & t \leq \tau, \\ F_{i,t}^{\text{mask}}(x, y), & t > \tau. \end{cases} \quad (6)$$

This scheme accurately tracks the motion encoded by the mask sequence, preserves high quality details, and generalizes across architectures, yielding consistent gains in multi subject scenarios.

4 EXPERIMENTS

Datasets. To comprehensively evaluate the effectiveness of multi-subject video editing methods in complex scenarios, we construct MSVBench. In this benchmark, over 60% of videos contain three or more subjects. It consists of 100 videos collected from YouTube³ and TikTok⁴, covering diverse subjects such as humans, animals, and vehicles, and intentionally includes multi-subject cases that are underrepresented in existing datasets. The number of subjects per video ranges from one to

³<https://www.youtube.com>

⁴<https://www.tiktok.com>

more than ten. For captions and editing prompts, we employ GPT-4o (Achiam et al., 2023) to generate scene descriptions for each video and automatically produce corresponding editing instructions based on subject attributes. All generated descriptions and prompts are manually verified to ensure accuracy and usability. Further details are provided in Appendix A.

Metrics. Following (Cong et al., 2023; Yang et al., 2025), we evaluate video editing fidelity using four metrics. Specifically, Warp-Err quantifies background consistency in non-edited regions. CLIP-T measures the alignment between the edited text and the edited regions; CLIP-F assesses perceptual consistency between adjacent frames. Moreover, Q-Edit is a composite indicator that reflects text alignment and temporal consistency. In addition, to assess spatial consistency before and after editing under varying numbers of subjects, we present center matching error (CM-Err), which performs one-to-one matching of subject boxes detected by GroundingDINO (Liu et al., 2024b) before and after editing and computes the mean center displacement. More details are provided in Appendix B.

Implementation Details. All experiments are conducted on a single NVIDIA A800 80 GB GPU. Unless stated otherwise, the configuration is as follows: (i) the denoising DiT and the conditional DiT are initialized from the pre-trained Wan2.1 (Jiang et al., 2025); (ii) the text to image model is the pre-trained SDXL (Podell et al., 2023), and the vision language model is Qwen2.5 VL 32B Instruct (Bai et al., 2023); (iii) instance masks are obtained using Grounded SAM 2 (Ren et al., 2024), and depth maps are estimated with Depth Anything V2 (Yang et al., 2024a); (iv) at inference we use 50 denoising steps and set the injection threshold to $\tau = 30$.

4.1 MAIN RESULTS

We compare our proposed IMAGEdit with several state-of-the-art methods, including open-source approaches such as FateZero (Qi et al., 2023), TokenFlow (Geyer et al., 2023), VideoPainter (Bian et al., 2025), VideoGrain (Yang et al., 2025), and DMT (Yatim et al., 2024), as well as closed-source approaches such as Keling⁵, Runway⁶, and Viggle⁷.

Quantitative Results. On MSVBench, the proposed IMAGEdit delivers consistently superior performance across all key metrics from Table 1. Concretely, it achieves the best scores with Warp-Err (1.85), CLIP-T (27.23), CLIP-F (97.93), Q-Edit (14.72), and CM-Err (2.83). Compared with the strongest open-source methods, IMAGEdit improves Q-Edit from 13.13 (DMT) to 14.72 (+12.1%), evidencing the benefit of robust multimodal features from the prompt-guided multimodal alignment for edit fidelity. Meanwhile, it reduces CM-Err from 3.12 (VideoGrain) to 2.83 while slightly lowering Warp-Err from 1.87 (DMT) to 1.85, demonstrating that the precise masks produced by the prior-based mask retargeting improve temporal consistency and background preservation. Even against closed-source methods, IMAGEdit remains competitive, e.g., Q-Edit 14.72 vs. 13.81 (Runway). Overall, these results substantiate the effectiveness of our proposed IMAGEdit.

Qualitative Results. From Figure 7, most competing methods (e.g., FateZero, TokenFlow, and VideoGrain) suffer from boundary entanglement and attention dilution, often leading to incomplete edits, background corruption, or attribute leakage across subjects. In contrast, IMAGEdit correctly transforms the designated subjects while preserving non-target regions, indicating that the prompt-guided multimodal alignment supplies robust multimodal conditions that precisely drive subject conversion. Moreover, existing approaches exhibit poor temporal stability under limb motions and occlusions, methods such as VideoPainter and DMT frequently show missing subjects or reduced fidelity, whereas our prior-based mask retargeting produces consistent mask sequences, enabling

Table 1: Quantitative results on MSVBench comparing IMAGEdit with SOTA methods. The best score is in **bold**; the second-best is underlined. A superscript * denotes closed-source methods.

Methods	Warp-Err ↓	CLIP-T ↑	CLIP-F ↑	Q-Edit ↑	CM-Err ↓
FateZero	2.16	24.26	<u>97.42</u>	11.23	3.49
TokenFlow	2.10	<u>26.57</u>	96.93	12.65	3.78
VideoPainter	2.05	24.13	96.97	11.77	4.70
VideoGrain	1.98	24.71	97.13	12.48	<u>3.12</u>
DMT	<u>1.87</u>	24.55	96.76	<u>13.13</u>	3.80
Keling*	2.00	25.66	98.37	12.83	4.39
Runway*	1.87	25.82	97.73	13.81	3.36
Viggle*	1.86	25.04	97.53	13.46	3.43
IMAGEdit	1.85	27.23	97.93	14.72	2.83

⁵<https://klingai.com/global>

⁶<https://runwayml.com>

⁷<https://viggle.ai>

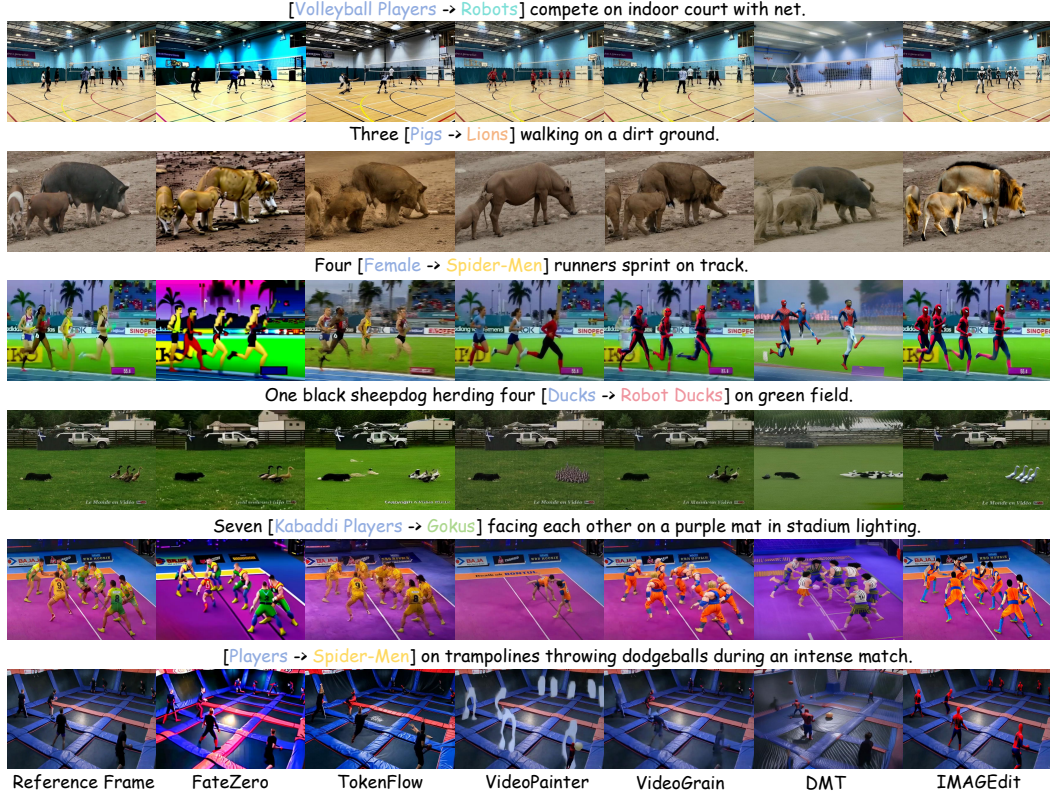


Figure 7: Qualitative comparison with SOTA video editing methods on MSVBench.

IMAGEdit to maintain frame-to-frame coherence and high fidelity under complex motion. Overall, our method yields more consistent and realistic edits, demonstrating the advantages of IMAGEdit.

User Study. The obtained quantitative and qualitative results underscore the substantial superiority of our IMAGEdit in generating results. To further validate the superiority of our method in human perception, we randomly selected 20 cases and recruited 20 volunteers to assess each method across three critical dimensions: Background Preservation (BP), Text Alignment (TA), and Video Quality (VQ). The volunteers ranked the edited videos according to these criteria to ensure a fair and comprehensive comparison across methods. As shown in Figure 8, IMAGEdit achieved the highest scores in BP, TA, and VQ, demonstrating its strong editing capability on videos with varying numbers of subjects.

4.2 ABLATION STUDY

To assess the effectiveness of each component, we construct the following variants within the IMAGEdit framework, keeping all other settings fixed while altering component configurations: **B0**: the base video generation model only Wan2.1. **B1**: only the prior-based mask retargeting module enabled. **B2**: only the prompt-guided multimodal alignment module enabled.

Prompt-Guided Multimodal Alignment. As shown in Table 2, adding the prompt-guided multimodal alignment module (B2) already improves performance over the base model (B0), increasing CLIP-T from 24.78 to 26.12 and Q-Edit from 13.24 to 14.04, while reducing CM-Err from 3.00 to 2.99. These improvements demonstrate that explicit alignment between textual prompts and visual priors provides stronger multimodal conditioning, leading to better adherence to

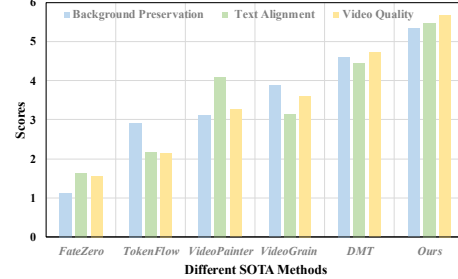


Figure 8: User study results. Higher values in these three metrics indicate better performance.

Table 2: Quantitative ablation results.

Methods	CLIP-T \uparrow	Q-Edit \uparrow	CM-Err \downarrow
B0	24.78	13.24	3.00
B1	25.10	13.42	2.87
B2	26.12	14.04	2.99
IMAGEdit	27.23	14.72	2.83

editing instructions and more consistent layouts. Visual comparisons are presented in Figure 9, it confirms that this module mitigates incomplete edits and attribute leakage, producing more accurate transformations across multiple subjects.

Prior-Based Mask Retargeting. From Table 2, incorporating the prior-based mask retargeting module (B1) yields clear improvements over the base model (B0), raising CLIP-T from 24.78 to 25.10 and Q-Edit from 13.24 to 13.42. Although CM-Err remains comparable, the generated masks are more precise and temporal consistent, enabling edits to better follow the target subjects across frames. Figure 9 further shows that this module effectively reduces boundary entanglement and preserves non-target regions, leading to more stable and faithful video edits, particularly in multi-subject scenarios with dense interactions or occlusions.

4.3 MORE RESULTS

Attention Weight Distribution. As shown in Figure 10, we systematically evaluated the impact of prompt-guided multimodal alignment on the spatial distribution of cross-attention weights. The target prompt is “Two Iron-Men are playing tennis on a tennis court.” We visualized the cross-attention of “Iron-Men” to assess the weight distribution. Without prompt-guided multimodal alignment, the attention weight for “Iron-Men” appears only in certain areas, such as the head, leading to incomplete editing. In contrast, IMAGEDit evenly distributes the attention weight for “Iron-Men” across the entire body, which is correct. This is because prompt-guided multimodal alignment provides multimodal conditional information, allowing for better capture of the regions that need editing.



Figure 9: Visualization of ablation results of IMAGEDit. (People → Super Mario)

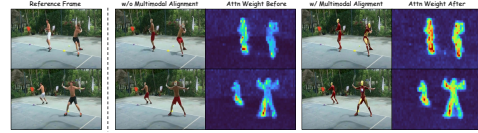


Figure 10: Attention weight distribution for both without (w/o) and with (w/) multimodal condition. (Players → Iron-Men)



Figure 11: Results across multiple scenarios, demonstrating the extensibility of IMAGEDit.

Multi-Scenario Applications. IMAGEDit also performs strongly across diverse application scenarios, including subject wise category specific editing, fine grained editing, and background editing. Specifically, as shown in Figure 11 (a), we convert the left person into an ultraman and the right person into a robot; Figure 11 (b) demonstrates fine grained edits such as adding glasses and changing clothing; Figure 11 (c) edits the background to Autumn Forest, snowy forest, and starry sky styles. Overall, IMAGEDit maintains stable appearance and clean boundaries, indicating good scalability of the framework. Additional results are provided in Appendix C.

5 CONCLUSION

We presented IMAGEDit, a training free framework for video editing with any number of subjects that changes designated categories. IMAGEDit provides robust multimodal conditioning and precise mask motion sequences through two key components, a prompt guided multimodal alignment module and a prior based mask retargeting module. By leveraging the understanding and generation capabilities of large pretrained models, these components produce aligned multimodal signals and time consistent masks that effectively remedy insufficient prompt side conditioning and overcome mask boundary entanglement in crowded scenes. The framework then conditions a pretrained mask driven video generator to synthesize the edited video. IMAGEDit is plug and play with a wide range of mask driven backbones and consistently improves overall performance. Extensive experiments on the new multi subject benchmark MSVBench verify that IMAGEDit surpasses state of the art methods. Code, dataset, and weights will be released to support further research.

REFERENCES

Josh Achiam, Steven Adler, Sandhini Agarwal, Lama Ahmad, Ilge Akkaya, Florencia Leoni Aleman, Diogo Almeida, Janko Altenschmidt, Sam Altman, Shyamal Anadkat, et al. Gpt-4 technical report. *arXiv preprint arXiv:2303.08774*, 2023.

Jinze Bai, Shuai Bai, Shusheng Yang, Shijie Wang, Sinan Tan, Peng Wang, Junyang Lin, Chang Zhou, and Jingren Zhou. Qwen-vl: A versatile vision-language model for understanding, localization, text reading, and beyond, 2023. URL <https://arxiv.org/abs/2308.12966>.

Yuxuan Bian, Zhaoyang Zhang, Xuan Ju, Mingdeng Cao, Liangbin Xie, Ying Shan, and Qiang Xu. Videopainter: Any-length video inpainting and editing with plug-and-play context control. In *Proceedings of the Special Interest Group on Computer Graphics and Interactive Techniques Conference Conference Papers*, pp. 1–12, 2025.

Duygu Ceylan, Chun-Hao P Huang, and Niloy J Mitra. Pix2video: Video editing using image diffusion. In *Proceedings of the IEEE/CVF International Conference on Computer Vision*, pp. 23206–23217, 2023.

Junsong Chen, Jincheng Yu, Chongjian Ge, Lewei Yao, Enze Xie, Yue Wu, Zhongdao Wang, James Kwok, Ping Luo, Huchuan Lu, et al. Pixart-alpha: Fast training of diffusion transformer for photorealistic text-to-image synthesis. *arXiv preprint arXiv:2310.00426*, 2023.

Zhe Chen, Jiannan Wu, Wenhui Wang, Weijie Su, Guo Chen, Sen Xing, Muyan Zhong, Qinglong Zhang, Xizhou Zhu, Lewei Lu, et al. Internvl: Scaling up vision foundation models and aligning for generic visual-linguistic tasks. In *Proceedings of the IEEE/CVF conference on computer vision and pattern recognition*, pp. 24185–24198, 2024.

Bowen Cheng, Alex Schwing, and Alexander Kirillov. Per-pixel classification is not all you need for semantic segmentation. *Advances in neural information processing systems*, 34:17864–17875, 2021.

Bowen Cheng, Ishan Misra, Alexander G Schwing, Alexander Kirillov, and Rohit Girdhar. Masked-attention mask transformer for universal image segmentation. In *Proceedings of the IEEE/CVF conference on computer vision and pattern recognition*, pp. 1290–1299, 2022.

Hyung Won Chung, Noah Constant, Xavier Garcia, Adam Roberts, Yi Tay, Sharan Narang, and Orhan Firat. Unimax: Fairer and more effective language sampling for large-scale multilingual pretraining. *arXiv preprint arXiv:2304.09151*, 2023.

Yuren Cong, Mengmeng Xu, Christian Simon, Shoufa Chen, Jiawei Ren, Yanping Xie, Juan-Manuel Perez-Rua, Bodo Rosenhahn, Tao Xiang, and Sen He. Flatten: optical flow-guided attention for consistent text-to-video editing. *arXiv preprint arXiv:2310.05922*, 2023.

Jeff Donahue, Philipp Krähenbühl, and Trevor Darrell. Adversarial feature learning. *arXiv preprint arXiv:1605.09782*, 2016.

Xin Gao, Li Hu, Siqi Hu, Mingyang Huang, Chaonan Ji, Dechao Meng, Jinwei Qi, Penchong Qiao, Zhen Shen, Yafei Song, et al. Wan-s2v: Audio-driven cinematic video generation. *arXiv preprint arXiv:2508.18621*, 2025.

Michal Geyer, Omer Bar-Tal, Shai Bagon, and Tali Dekel. Tokenflow: Consistent diffusion features for consistent video editing. *arXiv preprint arXiv:2307.10373*, 2023.

Ian Goodfellow, Jean Pouget-Abadie, Mehdi Mirza, Bing Xu, David Warde-Farley, Sherjil Ozair, Aaron Courville, and Yoshua Bengio. Generative adversarial networks. *Communications of the ACM*, 63(11):139–144, 2020.

Yuwei Guo, Ceyuan Yang, Anyi Rao, Zhengyang Liang, Yaohui Wang, Yu Qiao, Maneesh Agrawala, Dahua Lin, and Bo Dai. Animatediff: Animate your personalized text-to-image diffusion models without specific tuning. *arXiv preprint arXiv:2307.04725*, 2023.

Kaiming He, Georgia Gkioxari, Piotr Dollár, and Ross Girshick. Mask r-cnn. In *Proceedings of the IEEE international conference on computer vision*, pp. 2961–2969, 2017.

Jonathan Ho, William Chan, Chitwan Saharia, Jay Whang, Ruiqi Gao, Alexey Gritsenko, Diederik P Kingma, Ben Poole, Mohammad Norouzi, David J Fleet, et al. Imagen video: High definition video generation with diffusion models. *arXiv preprint arXiv:2210.02303*, 2022.

Wenyi Hong, Ming Ding, Wendi Zheng, Xinghan Liu, and Jie Tang. Cogvideo: Large-scale pre-training for text-to-video generation via transformers. *arXiv preprint arXiv:2205.15868*, 2022.

Zeyinzi Jiang, Zhen Han, Chaojie Mao, Jingfeng Zhang, Yulin Pan, and Yu Liu. Vace: All-in-one video creation and editing. *arXiv preprint arXiv:2503.07598*, 2025.

Diederik P Kingma and Max Welling. Auto-encoding variational bayes. *arXiv preprint arXiv:1312.6114*, 2013.

Alexander Kirillov, Eric Mintun, Nikhila Ravi, Hanzi Mao, Chloe Rolland, Laura Gustafson, Tete Xiao, Spencer Whitehead, Alexander C. Berg, Wan-Yen Lo, Piotr Dollár, and Ross Girshick. Segment anything. *arXiv:2304.02643*, 2023.

Max Ku, Cong Wei, Weiming Ren, Harry Yang, and Wenhui Chen. Anyv2v: A tuning-free framework for any video-to-video editing tasks. *arXiv preprint arXiv:2403.14468*, 2024.

Yi Li, Haozhi Qi, Jifeng Dai, Xiangyang Ji, and Yichen Wei. Fully convolutional instance-aware semantic segmentation. In *Proceedings of the IEEE conference on computer vision and pattern recognition*, pp. 2359–2367, 2017.

Yitong Li, Martin Min, Dinghan Shen, David Carlson, and Lawrence Carin. Video generation from text. In *Proceedings of the AAAI conference on artificial intelligence*, volume 32, 2018.

Shaoteng Liu, Yuechen Zhang, Wenbo Li, Zhe Lin, and Jiaya Jia. Video-p2p: Video editing with cross-attention control. In *Proceedings of the IEEE/CVF Conference on Computer Vision and Pattern Recognition*, pp. 8599–8608, 2024a.

Shilong Liu, Zhaoyang Zeng, Tianhe Ren, Feng Li, Hao Zhang, Jie Yang, Qing Jiang, Chunyuan Li, Jianwei Yang, Hang Su, et al. Grounding dino: Marrying dino with grounded pre-training for open-set object detection. In *European conference on computer vision*, pp. 38–55. Springer, 2024b.

Gaurav Mittal, Tanya Marwah, and Vineeth N Balasubramanian. Sync-draw: Automatic video generation using deep recurrent attentive architectures. In *Proceedings of the 25th ACM international conference on Multimedia*, pp. 1096–1104, 2017.

Augustus Odena, Christopher Olah, and Jonathon Shlens. Conditional image synthesis with auxiliary classifier gans. In *International conference on machine learning*, pp. 2642–2651. PMLR, 2017.

Yingwei Pan, Zhaofan Qiu, Ting Yao, Houqiang Li, and Tao Mei. To create what you tell: Generating videos from captions. In *Proceedings of the 25th ACM international conference on Multimedia*, pp. 1789–1798, 2017.

William Peebles and Saining Xie. Scalable diffusion models with transformers. In *Proceedings of the IEEE/CVF international conference on computer vision*, pp. 4195–4205, 2023.

Dustin Podell, Zion English, Kyle Lacey, Andreas Blattmann, Tim Dockhorn, Jonas Müller, Joe Penna, and Robin Rombach. Sdxl: Improving latent diffusion models for high-resolution image synthesis. *arXiv preprint arXiv:2307.01952*, 2023.

Chenyang Qi, Xiaodong Cun, Yong Zhang, Chenyang Lei, Xintao Wang, Ying Shan, and Qifeng Chen. Fatezero: Fusing attentions for zero-shot text-based video editing. In *Proceedings of the IEEE/CVF International Conference on Computer Vision*, pp. 15932–15942, 2023.

Yurui Qian, Qi Cai, Yingwei Pan, Yehao Li, Ting Yao, Qibin Sun, and Tao Mei. Boosting diffusion models with moving average sampling in frequency domain. In *Proceedings of the IEEE/CVF conference on computer vision and pattern recognition*, pp. 8911–8920, 2024.

Alec Radford, Luke Metz, and Soumith Chintala. Unsupervised representation learning with deep convolutional generative adversarial networks. *arXiv preprint arXiv:1511.06434*, 2015.

Aditya Ramesh, Prafulla Dhariwal, Alex Nichol, Casey Chu, and Mark Chen. Hierarchical text-conditional image generation with clip latents. *arXiv preprint arXiv:2204.06125*, 1(2):3, 2022.

Nikhila Ravi, Valentin Gabeur, Yuan-Ting Hu, Ronghang Hu, Chaitanya Ryali, Tengyu Ma, Haitham Khedr, Roman Rädl, Chloe Rolland, Laura Gustafson, et al. Sam 2: Segment anything in images and videos. *arXiv preprint arXiv:2408.00714*, 2024.

Shaoqing Ren, Kaiming He, Ross Girshick, and Jian Sun. Faster r-cnn: Towards real-time object detection with region proposal networks. *IEEE transactions on pattern analysis and machine intelligence*, 39(6):1137–1149, 2016.

Tianhe Ren, Shilong Liu, Ailing Zeng, Jing Lin, Kunchang Li, He Cao, Jiayu Chen, Xinyu Huang, Yukang Chen, Feng Yan, et al. Grounded sam: Assembling open-world models for diverse visual tasks. *arXiv preprint arXiv:2401.14159*, 2024.

Robin Rombach, Andreas Blattmann, Dominik Lorenz, Patrick Esser, and Björn Ommer. High-resolution image synthesis with latent diffusion models. In *Proceedings of the IEEE/CVF conference on computer vision and pattern recognition*, pp. 10684–10695, 2022.

Olaf Ronneberger, Philipp Fischer, and Thomas Brox. U-net: Convolutional networks for biomedical image segmentation. In *International Conference on Medical image computing and computer-assisted intervention*, pp. 234–241. Springer, 2015.

Carsten Rother, Vladimir Kolmogorov, and Andrew Blake. ” grabcut” interactive foreground extraction using iterated graph cuts. *ACM transactions on graphics (TOG)*, 23(3):309–314, 2004.

Nataniel Ruiz, Yuanzhen Li, Varun Jampani, Yael Pritch, Michael Rubinstein, and Kfir Aberman. Dreambooth: Fine tuning text-to-image diffusion models for subject-driven generation. In *Proceedings of the IEEE/CVF conference on computer vision and pattern recognition*, pp. 22500–22510, 2023.

Fei Shen, Xiaoyu Du, Yutong Gao, Jian Yu, Yushe Cao, Xing Lei, and Jinhui Tang. Imagharmony: Controllable image editing with consistent object quantity and layout. *arXiv preprint arXiv:2506.01949*, 2025.

Uriel Singer, Adam Polyak, Thomas Hayes, Xi Yin, Jie An, Songyang Zhang, Qiyuan Hu, Harry Yang, Oron Ashual, Oran Gafni, et al. Make-a-video: Text-to-video generation without text-video data. *arXiv preprint arXiv:2209.14792*, 2022.

Team Wan, Ang Wang, Baole Ai, Bin Wen, Chaojie Mao, Chen-Wei Xie, Di Chen, Feiwu Yu, Haiming Zhao, Jianxiao Yang, et al. Wan: Open and advanced large-scale video generative models. *arXiv preprint arXiv:2503.20314*, 2025.

Peng Wang, Shuai Bai, Sinan Tan, Shijie Wang, Zhihao Fan, Jinze Bai, Keqin Chen, Xuejing Liu, Jialin Wang, Wenbin Ge, et al. Qwen2-vl: Enhancing vision-language model’s perception of the world at any resolution. *arXiv preprint arXiv:2409.12191*, 2024.

Yukun Wang, Longguang Wang, Zhiyuan Ma, Qibin Hu, Kai Xu, and Yulan Guo. Videodirector: Precise video editing via text-to-video models. In *Proceedings of the Computer Vision and Pattern Recognition Conference*, pp. 2589–2598, 2025.

Jay Zhangjie Wu, Yixiao Ge, Xintao Wang, Stan Weixian Lei, Yuchao Gu, Yufei Shi, Wynne Hsu, Ying Shan, Xiaohu Qie, and Mike Zheng Shou. Tune-a-video: One-shot tuning of image diffusion models for text-to-video generation. In *Proceedings of the IEEE/CVF international conference on computer vision*, pp. 7623–7633, 2023.

Wei Wu, Qingnan Fan, Shuai Qin, Hong Gu, Ruoyu Zhao, and Antoni B Chan. Freediff: Progressive frequency truncation for image editing with diffusion models. In *European Conference on Computer Vision*, pp. 194–209. Springer, 2024.

Lihe Yang, Bingyi Kang, Zilong Huang, Zhen Zhao, Xiaogang Xu, Jiashi Feng, and Hengshuang Zhao. Depth anything v2, 2024a. URL <https://arxiv.org/abs/2406.09414>.

Xiangpeng Yang, Linchao Zhu, Hehe Fan, and Yi Yang. Videograin: Modulating space-time attention for multi-grained video editing. In *The Thirteenth International Conference on Learning Representations*, 2025.

Zhuoyi Yang, Jiayan Teng, Wendi Zheng, Ming Ding, Shiyu Huang, Jiazheng Xu, Yuanming Yang, Wenyi Hong, Xiaohan Zhang, Guanyu Feng, et al. Cogvideox: Text-to-video diffusion models with an expert transformer. *arXiv preprint arXiv:2408.06072*, 2024b.

Danah Yatim, Rafail Fridman, Omer Bar-Tal, Yoni Kasten, and Tali Dekel. Space-time diffusion features for zero-shot text-driven motion transfer. In *Proceedings of the IEEE/CVF Conference on Computer Vision and Pattern Recognition*, pp. 8466–8476, 2024.

Shengming Yin, Chenfei Wu, Jian Liang, Jie Shi, Houqiang Li, Gong Ming, and Nan Duan. Drag-nuwa: Fine-grained control in video generation by integrating text, image, and trajectory. *arXiv preprint arXiv:2308.08089*, 2023.

Dong Zhang, Lingfeng He, Rui Yan, Fei Shen, and Jinhui Tang. R-genie: Reasoning-guided generative image editing. *arXiv preprint arXiv:2505.17768*, 2025.

Lvmin Zhang, Anyi Rao, and Maneesh Agrawala. Adding conditional control to text-to-image diffusion models. In *Proceedings of the IEEE/CVF international conference on computer vision*, pp. 3836–3847, 2023.

Wenwei Zhang, Jiangmiao Pang, Kai Chen, and Chen Change Loy. K-net: Towards unified image segmentation. *Advances in Neural Information Processing Systems*, 34:10326–10338, 2021.

SUPPLEMENTARY MATERIAL

This supplementary material provides extended details for the methodology and experiments presented in the main paper. Section A details the MSVBench dataset. Section B describes the computation of the CM-Err metric. Section C reports additional results, including evaluations on extra datasets, broader qualitative comparisons, and further examples of scalable applications. Section D discusses potential avenues for future research.



Figure 12: Display of randomly selected samples from the MSVBench dataset.

A MSVBENCH DATASET

To fill the evaluation gap in multi subject video editing, we construct MSVBench with 100 videos, more than sixty percent of which contain three or more subjects, as shown in Figure 12. Videos are primarily sourced from YouTube and TikTok. Scenes cover humans, animals, and vehicles; the number of subjects per frame ranges from one to more than ten, and the dataset includes challenging cases with crowded layouts, strong occlusions and interactions, significant camera motion, and complex backgrounds. Unlike prior editing datasets that focus on single subject or face centered clips, MSVBench is explicitly sampled and annotated around high subject count, dense layouts, and interaction or occlusion ordering, making it well suited to evaluate category fidelity, layout preservation, and boundary leakage. For annotation, GPT-4o (Achiam et al., 2023) generates concise video level descriptions and corresponding editing prompts, which are then verified by human annotators for accuracy and consistency; Grounded SAM2 (Ren et al., 2024) produces instance level masks for the target regions, followed by manual checks to ensure temporal consistency. We will release the verified descriptions and prompts, mask sequences, and evaluation scripts, and we report the distribution of subject counts in Figure 13 to facilitate reproduction and comparison.

B CENTER MATCHING ERROR METRIC

We assess subject count and layout consistency before and after editing with a layout aware, alignment free metric, since pixel overlap measures such as mIoU cannot capture merges, splits, or relocations. We introduce center matching error (CM-Err). For frame t of width W and height H , let $\mathcal{A}_t = \{a_j\}$ and $\mathcal{B}_t = \{b_k\}$ be the sets of bounding boxes from the original and edited frames. For a box $b = (x_{\min}, y_{\min}, x_{\max}, y_{\max})$, its center is $c(b) = ((x_{\min} + x_{\max})/2, (y_{\min} + y_{\max})/2)$. The normalized center distance between a_j and b_k is

$$d_{jk}^{(t)} = \frac{\|c(a_j) - c(b_k)\|_2}{\sqrt{W^2 + H^2}} \in [0, 1]. \quad (7)$$

Using $d_{jk}^{(t)}$ as the cost, we compute the minimal one to one matching between \mathcal{A}_t and \mathcal{B}_t ; let M_t be the number of matched pairs and $U_t = |\mathcal{A}_t| + |\mathcal{B}_t| - 2M_t$ the number of unmatched boxes. The frame level error is

$$\text{CM-Err}^{(t)} = \frac{\sum_{i=1}^{M_t} d_i^{(t)} + U_t}{M_t + U_t}, \quad (8)$$

where $d_i^{(t)}$ is the normalized distance of the i th matched pair and each unmatched box incurs a unit penalty. For a video with T frames, the score is

$$\text{CM-Err} = \frac{1}{T} \sum_{t=1}^T \text{CM-Err}^{(t)}. \quad (9)$$

Lower values indicate better preservation of subject count and center locations, while higher values reflect additions or removals of subjects, merges or splits, and spatial displacements.

C EXPERIMENTS

Table 3: Comparison of different video editing methods on loveu-tgve-2023.

Methods	Warp-Err ↓	CLIP-T ↑	CLIP-F ↑	Q>Edit ↑	CM-Err ↓
VideoGrain (Yang et al., 2025)	2.14	25.22	96.78	11.78	3.05
TokenFlow (Geyer et al., 2023)	2.23	24.22	97.20	10.86	3.54
FateZero (Qi et al., 2023)	2.18	23.80	97.11	10.91	3.75
DMT (Yatim et al., 2024)	1.90	23.82	97.18	12.53	3.61
VideoPainter (Bian et al., 2025)	2.12	22.95	95.95	10.82	4.04
IMAGEDit	<u>2.04</u>	25.99	97.23	12.74	2.66

The loveu-tgve-2023 Dataset Results. As noted above, we achieved strong results on the proposed MSVBench. To further validate our method, we also evaluate on the loveu-tgve-2023 dataset, where more than 80% of samples contain single or few subjects. As shown in Table 3, IMAGEDit attains the best semantic consistency and editing quality (CLIP-T 25.99, CLIP-F 97.23, Q-Edit 12.74) and the best layout and count preservation (lowest CM-Err 2.66), indicating better retention of category fidelity, subject centers, and counts after editing. For temporal and geometric stability, Warp-Err reaches 2.04, second only to DMT at 1.90, placing IMAGEDit in the leading group and balancing low distortion with high quality. Compared with VideoGrain and TokenFlow, IMAGEDit shows more balanced gains across metrics, demonstrating strong generalization and consistency in single or few subject scenarios.

The Influence of τ . We vary the injection threshold τ from 0 to 50 to study how long the mask motion sequence should guide the denoising process. As shown in Figure 14, very small values of τ provide insufficient structural guidance, leading to boundary leakage, imperfect occlusion ordering, and occasional identity drift. In contrast, very large values inject fusion signals into late refinement steps and introduce artifacts such as texture corruption and visible seams. Mid range settings yield a better balance: around $\tau = 30$ the edits preserve structure and layering while allowing the backbone to synthesize high frequency details, producing clean boundaries and stable appearance. We therefore set $\tau = 30$ based on cross validation on a held out split.

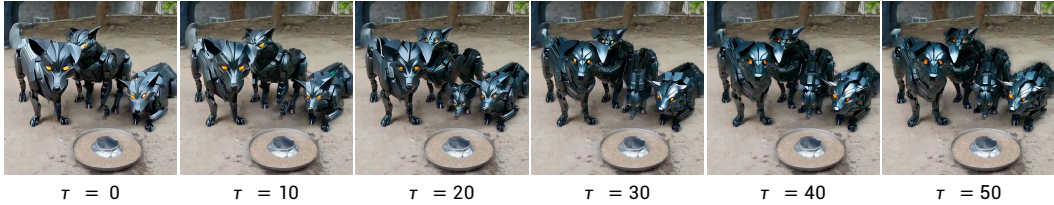


Figure 14: Ablation on τ . The parameter τ is varied between 0 and 50 to systematically examine its effects. We show the last frame of the edit video.

More Qualitative Results. Figure 15 presents additional side by side comparisons on continuous frames, covering fast motion, crowded scenes, and multi subject counts. Compared with baseline, IMAGEDit preserves category fidelity and identity consistency, produces cleaner boundaries, and yields edits with better temporal consistency, with fewer leakage artifacts and less flicker.

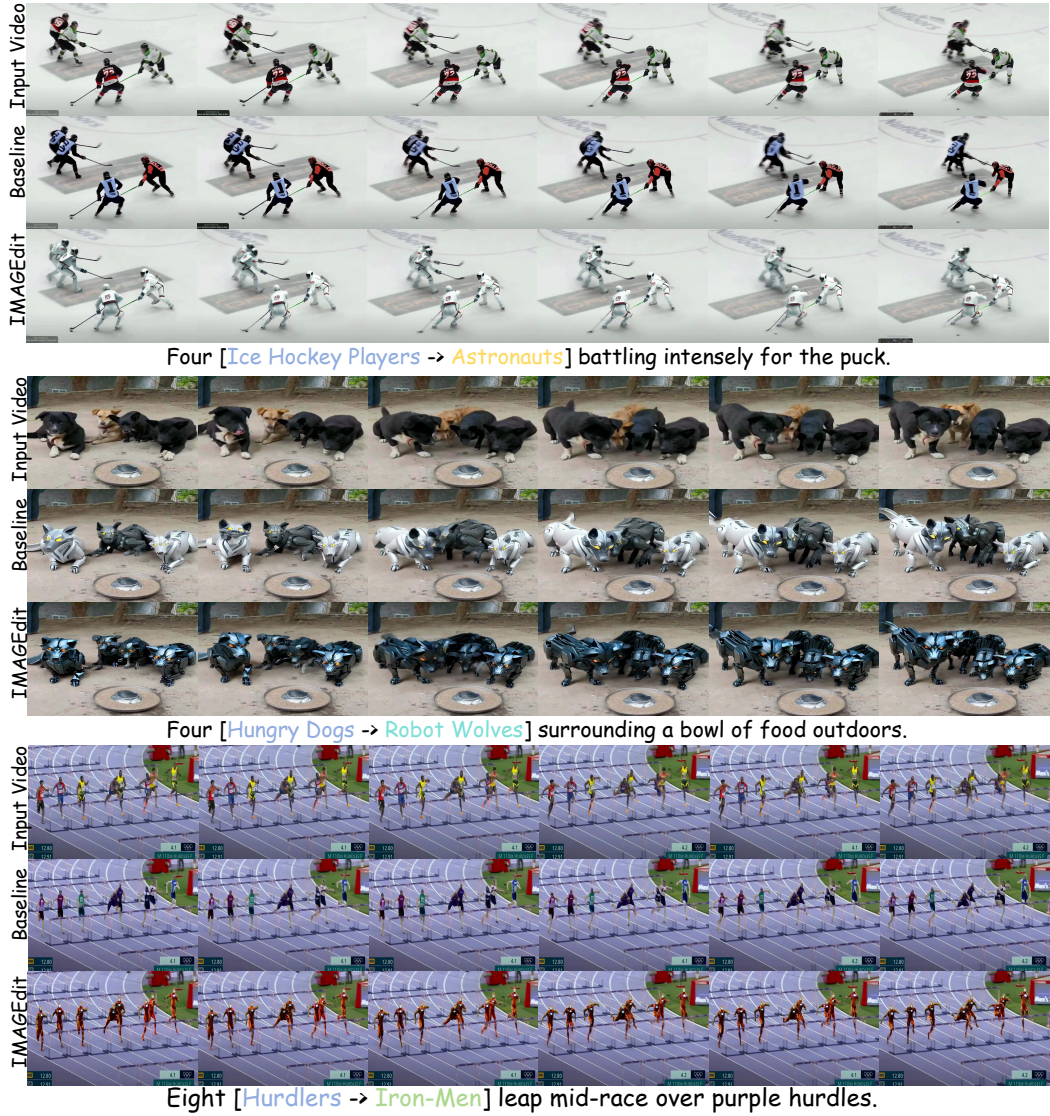


Figure 15: More qualitative comparisons between IMAGEEdit and baseline methods on the MSVBench dataset.

More Applications Results. Figure 16 showcases the extensible applications of IMAGEEdit across diverse scenarios, including (a) background editing, (b) multi round editing, (c) specified subject editing, (d) long video editing, (e) face swapping, (f) partial editing, (g) clothing swapping, and (h) viewpoint change editing. These results indicate that IMAGEEdit preserves non-target regions and maintains strong temporal consistency across tasks and complex scenes without fine-tuning.

D FUTURE WORK

Although IMAGEEdit has demonstrated strong performance, future work can explore a parameterized motion and expression retargeting module built on latent diffusion representations. By driving subject level video editing with continuously controllable spatiotemporal parameters, we aim to further improve temporal consistency and editing accuracy in long horizon and heavy occlusion scenarios.

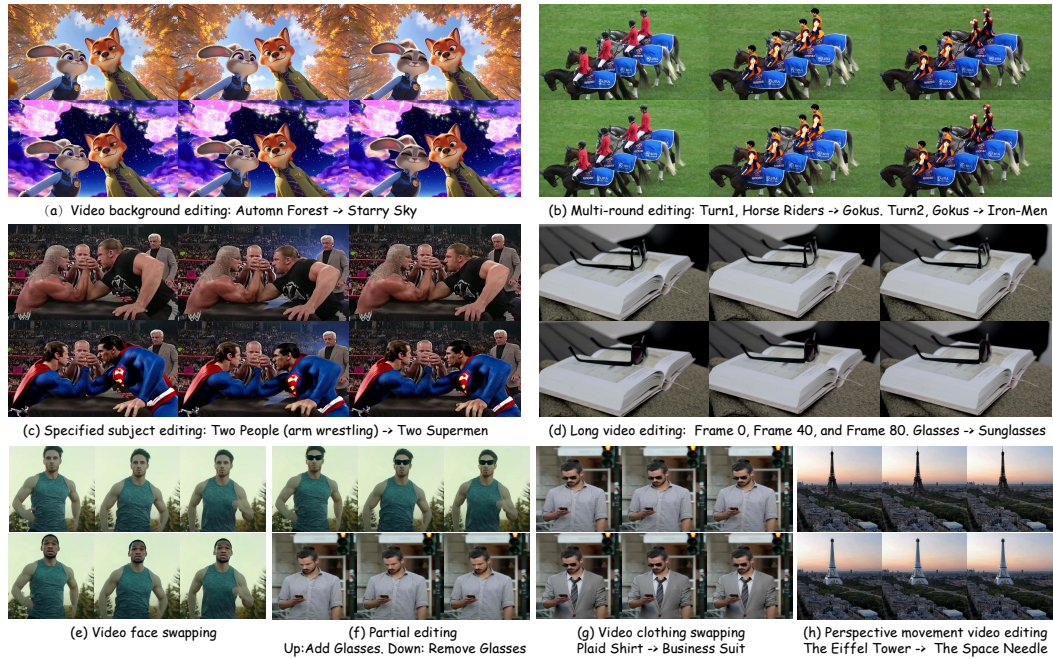


Figure 16: More qualitative comparisons on multi-scenario applications.